Old Dominion University Research Foundation

DEPARTMENT OF CIVIL ENGINEERING
COLLEGE OF ENGINEERING & TECHNOLOGY
OLD DOMINION UNIVERSITY
NORFOLK, VIRGINIA 23529

POLYMER INFILTRATION STUDIES

By

Joseph M. Marchello, Principal Investigator

Progress Report
For the period July 1, 1993 to September 30, 1993

Prepared for
National Aeronautics and Space Administration
Langley Research Center
Hampton, VA 23681-0001

Under
Research Grant NAG-1-1067
Robert M. Baucom, Technical Monitor
MD-Polymeric Materials Branch

September 1993

DEPARTMENT OF CIVIL ENGINEERING
COLLEGE OF ENGINEERING & TECHNOLOGY
OLD DOMINION UNIVERSITY
NORFOLK, VIRGINIA 23529

POLYMER INFILTRATION STUDIES

By

Joseph M. Marchello, Principal Investigator

Progress Report
For the period July 1, 1993 to September 30, 1993

Prepared for
National Aeronautics and Space Administration
Langley Research Center
Hampton, VA 23681-0001

Under
Research Grant NAG-1-1067
Robert M. Baucom, Technical Monitor
MD-Polymeric Materials Branch

Submitted by the
Old Dominion University Research Foundation
P.O. Box 6369
Norfolk, Virginia 23508-0369

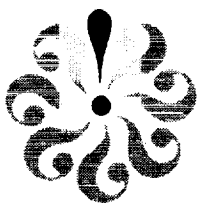

September 1993

POLYMER INFILTERATION STUDIES

Summary

During the past three months, significant progress has been made on the preparation of carbon fiber composities using advanced polymer resins. The results are set forth in recent reports and publications, and will be presented at forthcoming national and international meetings.

Current and ongoing research activities reported herein include:

- Textile Composites from Powder-Coated Towpreg: Role of Surface Coating in Braiding
- Prepregger hot sled operation
- Ribbonizing Powder-Impregenated Towpreg
- Textile Composites from Powder-Coated Towpreg: Role of Bulk Factor
- Powder Curtain Prepreg Process
- ATP Open-Section Part Warpage Control

During the coming months research will be directed toward further development of the new powder curtain pregregging method and on ways to customize dry powder towpreg for textile and robotic applications in aircraft part fabrication.

Studies of multi-tow powder prepregging and ribbon preparation will be conducted in conjunction with continued development of prepregging technology and the various aspects of composite part fabrication using customized towpreg. Also, during the period ahead work will continue on the analysis of the performance of the new solution prepregger.

Polymer Infilteration Studies

Polymer infilteration investigations are directed toward development of methods by which to produce advanced composite material for automated part fabrication utilizing textile and robotic technology in the manufacture of subsonic and supersonic aircraft. This object is to achieved through research investigations at NASA Langley Research Center and by stimulating technology transfer between contract researchers and the aircraft industry.

The powder curtain prepregging system, which was started up successfully last year has been used to produce over three hundred pounds of towpreg. It is currently undergoing modifications. The automated powder return system was contructed and is undergoing tests. Modification are being made to the powder curtain tube, for extended curtain width demonstration. These changes should provide better operating control over fugitive powder and improved towpreg quality control.

Issues in the use of powder coated towpreg for textile applications have been the subject of significant effort. Studies of ways to debulk powder preforms are being conducted, see attachments. Also, work has been initiated on use of gel coating to reduce tow-tow friction during braiding.

Consideration of the ways to customized towpreg for use in automated tow /fiber placement has resulted in several new approaches and will be the subject of a paper to be presented at the SAMPE. Noteworthy among the ideas that have been developed is the potential benefits from use of non-rectangular ribbon, and the thermal wave bonding model of tow placement with on-the-fly-cure, see attachmnent. Several efforts to produce quality towpreg ribbon are underway. In addition to die forming methods, it is planned to investigate making unitape from powdered tow which can then be slit into the desired ribbon geometry.

The following attachments provide detailed information about several current and planned research projects.

Attachments

1. Textile Composite from Powder-Coated Towpreg: Role of Bulk Factor During Consolidation: paper to bepresented at SAMPE Meeting In Philadelpia October 25.

2. ATP Thermal Wave Bonding Memorandum

TEXTILE COMPOSITES FROM POWDER-COATED TOWPREG: ROLE OF BULK FACTOR DURING CONSOLIDATION*

Maylene K. Hugh and Joseph M. Marchello
Old Dominion University
Norfolk, Virginia 23529

Robert M. Baucom and Norman J. Johnston
NASA Langley Research Center
Hampton, Virginia 23681-0001

ABSTRACT

To obtain good mechanical properties for textile composites a cure process is required that provides full consolidation of bulky, woven or braided preforms. Consolidation is a major concern, since bulk factors--the ratio of preform thickness to final part thickness--are on the order of five to one for powder-coated 2D textiles, and three to one for 3D textiles.

The role of bulk factor during consolidation was investigated. Carbon fiber (12k AS-4†, Hercules) coated with epoxy powder (AMD0029†, 3M Corporation) was woven into a T-stiffened panel structure using a 3D through-the-thickness weaving method developed by Techniweave, Inc. Full consolidation of the stiffened panel preform entailed a two-step process involving an initial debulking of the preform to obtain the gross fiber movement and wetting needed for the intimate contact of resin and fiber, followed by final consolidation to net shape. Movable hard tooling was used to achieve major debulking of the preform to approximate net shape. A standard autoclave process was applied to accomplish final net shape using a combination of hard and soft tooling.

KEYWORDS: Manufacturing/Fabrication/Processing; Powder-Coated Towpreg; Three-Dimensional Woven Composites.

---

† Use of trade names or manufacturers does not constitute an official endorsement, either expressed or implied, by the National Aeronautics and Space Administration.

1.0 INTRODUCTION

Production costs of composite parts for primary structures in subsonic and supersonic aircraft applications must be decreased from their present levels in order for wide-spread use of composite materials to occur. Developments in the fabrication of composite parts point toward cost reduction through increased automation. In conjunction with the development of automated fabrication techniques, NASA Langley Research Center (LaRC) has developed a method of prepregging carbon fiber with dry thermoplastic and thermosetting polymer powder [1].

These efforts at NASA LaRC have focused on two established technologies--textiles and robotics. In order to be used in these automated processes, powder-coated towpreg must be produced in the form of either a textile quality yarn or an advanced tow placement (ATP) quality ribbon. Past studies [2] have focused on developing a protocol for producing eight-harness satin woven fabrics from towpreg. This study deals with the consolidation of 2D and 3D woven textile preforms into composite parts.

By coupling powder-coated towpreg with existing, highly automated textile processes, the resulting impregnated fabrics, broad goods and preforms can be molded into parts. These combined fabrication processes may be an alternative to resin transfer molding (RTM) of dry preforms in cases where complex mold geometries and tightly fabricated preforms pose wet-out problems. The powder coating process may offer the only viable method of part fabrication if high melt viscosity polymers are required to obtain improved composite properties, such as thermal stability and/or fracture toughness. The primary issue in utilizing powder-coated preforms is the need for significant debulking during the consolidation process [3].

Studies by Carpenter and Colton on thermoplastic filament winding [4] have identified three consolidation mechanisms: bulk consolidation, matrix flow and fiber network deformation. With thermosets there is the additional step of cure to cross-link the polymer chains. These steps take place in sequence as the composite's thickness decreases to its final consolidation level.

Full consolidation of powder-coated textile preforms entails a two-step process involving an initial debulking of the preform to obtain the gross fiber movement and wetting needed for the intimate contact of resin and fiber, followed by final consolidation to net shape. For some composite parts, these steps may require different tooling. In these instances, methods of forming, such as rubber-molding, hydroforming, diaphragm forming, and matched die molding, can be used to achieve the initial debulking of the preform into approximate net shape. Final consolidation to net shape can then be accomplished by standard autoclave or heat-press procedures.

The consolidation mechanisms in powder-coated 2D and 3D textile preforms has been investigated by Bayha, et al [5]. Methods of consolidation have involved stepwise debulking of 3D reinforced specimens followed by autoclave final debulking and cure. Debulking trials were performed to determine how effective various pressure and temperature combinations were on reducing bulk in as-fabricated 2D and 3D parts.

In this study, the role of bulk factor during consolidation was demonstrated. Carbon fiber (12k, AS-4) coated with epoxy powder (AMD0029) was woven into a T-stiffened preform using a 3D through-the-thickness weaving method of Techniweave, Inc. Movable hard tooling in a heat press was used to achieve major debulking of the preform to approximate net shape. A standard autoclave process was used to accomplish final net shape by employing hard tooling coupled with high temperature expansion rubber.

2.0 CONSOLIDATION PROCESS

The debulking of preforms is part of an ongoing investigation. The change in thickness during consolidation is between 3 to 1 and 5 to 1 for textile preforms. Vacuum and autoclave pressure is applied to induce the resin flow, wetting of fibers, and fiber movement necessary to eliminate voids and fill the intra- and inter-tow spaces. Once the system is at temperature, the ramping of the pressure allows the fibers time to move into a compact arrangement with minimum fiber crimping and breakage, and provides time for resin flow and adhesion.

2.1 Initial Debulking The need to debulk is inherent in making parts from powered towpreg. Figure 1 illustrates the acquisition of bulk during the impregnation of the tow with powder particles. This volume change occurs regardless of the method of towpreg production, although prepregging by a dry technique generally yields a slightly higher bulk than when using a wet (e.g., slurry) technique. This phenomena is due to the fact that in the dry processes the tow is grossly spread, compared to its intial size, before the impregnation step.

The process of debulking a composite laminate prior to final consolidation is standard throughout the industry. Experience has shown that debulking increases the quality of a thermoset laminate. The debulk cycle removes air that becomes trapped between plies as they are laid down, with the result being both improved handling of the preform and ease of insertion into the tooling. Bulk factors present a technical problem while working with powder towpreg preforms. While bulk factors in this study were 3:1, typically, bulk factors run about 4:1 in powder towpreg preforms. Up to 5:1 ratios have been measured in 2D woven fabrics.

Two T-stiffened preforms were debulked in 3 steps. First, the skin of one part was debulked using flat tooling and placing the part in a hydraulic heat press which sits inside a vacuum chamber. The press was heated to 93°C (200°F). Once the platens reached temperature, the

chamber was evacuated and 690 kPa (100 psi) of pressure was applied to the part for 20 minutes. Figure 2 shows the experimental setup.

The stiffener of the part was then debulked in a similar manner, as is shown in figure 3. Flat tooling was applied to the part. The same initial debulking step was used for the stiffener as for the skin.

2.2 Final Consolidation For the final consolidation, the initially debulked part was bagged and placed in an autoclave. As shown in figure 4, hard tooling was placed on the top surface of the skin, along with a layer of expansion rubber to place pressure in the through-the-thickness direction of both the skin and the stiffener. A layer of high-temperature, high-elongation, polyimide film (Upilex-R† , Ube Industries) was placed between the part and the rubber to protect the composite.

The autoclave cure (fig. 5) consisted of evacuating the air from inside the bag around the part and increasing the temperature. Once the part temperature reached 149°C (300°F), the pressure was then increased to 690 kPa (100 psi) at a rate of 128 kPa/min. The part temperature was then increased to 177°C (350°F) and held at temperature and pressure for 120 minutes. A second temperature increase to 215°C (420°F) was executed and sustained for 60 more minutes. The part was cooled under full pressure.

3.0 RESULTS AND DISCUSSION

In previous work [5], it was found that the large surface area of the skin portion of the preform restricted the tool from sliding inward to the stiffener, preventing even application of tool pressure, which caused an uneven debulk of the vertical stiffening member. After final consolidation of the part, the cross-section of the skin/stiffener intersection was not symmetric about the center line, but, the thickness of the respective horizontal and vertical members of the part were within specification.

In this study two T-stiffened panel parts were consolidated. As shown in figure 6, the preliminary debulking of the preforms resulted in over a 2:1 reduction in thickness in the skin, whereas preliminary debulking in the stiffener resulted in only a 20% reduction. The final autoclave consolidated part showed a 2.9-fold reduction in panel thickness and a 2.6-fold reduction in stiffener thickness from the as-woven preform. The first part (AU1513) exhibited a dimple at the bottom of the skin at the skin/stiffener intersection (fig. 7). In addition, wrinkles were observed on the top surface of the skin (fig.8), which were caused by puckering of the Upilex-R.

For the second part (AU1524) greater care was used in aligning the tools for initial debulking and placing the tool, expansion rubber, and Upilex-R for the final autoclave consolidation

† Use of trade names or manufacturers does not constitute an official endorsement, either expressed or implied, by the National Aeronautics and Space Administration.

step. In addition, the part was placed on a steel caul plate to give the part a solid, hard surface to form against. This resulted in a good quality part (fig. 9). No wrinkles were found on the top surface and no dimple formed at the skin/stffener intersection.

Observations of the surface of the part indicated that during debulking, as the part thickness decreases, the z-direction fiber extends through the surface. Because of the presence of the tooling, the excess length of z-direction yarn flattens across the part surface, which may reduce the in-plane properties in the skin. On the other hand, since the excess z-fiber moved to the surface, the portion of the z-fiber remaining in the interior of the consolidated part may be straight, thereby providing through-the-thickness reinforcement. Future work will examine these microstructural phenomena.

This study has contributed to the understanding of ways to consolidate bulky powder-coated textile preforms. Through the stepwise debulking and consolidation process, preforms with initial bulk factors of 3 to 1 can be successfully consolidated. Future work on tooling development deals with two dimensional tool surface movement. This work is directed toward integrating the debulking and consolidation processes into a single step. Additional studies deal with application of the process to other part geometries and polymer systems.

4.0 ACKNOWLEDGMENTS

The authors gratefully acknowledge the assistance of Mr. John Snoha for preparing the powder-coated towpreg and the consolidated woven parts, Mr. Ricky Smith for coordinating the laboratory activities, and Mr. Scott Warrington for the computer graphics. This work was performed under NASA grant NAG1-1067 with Old Dominion University, Norfolk, VA.

5.0. REFERENCES

1. R. M. Baucom and J. M. Marchello, SAMPE International Symposium, 38, 1902, (1993).

2. M. K. Hugh, J. M. Marchello, R. M. Baucom and N. J. Johnston, SAMPE International Symposium, 36, 1040, (1992).

3. S. R. Iyer and L. T. Drzal, J. of Thermoplastic Composite Materials, 3, 325, (1990).

4. C. E. Carpenter and J. S. Colton, SAMPE International Symposium, 38, 205, (1993).

5. T. D. Bayha, P. P. Osborne, T. P. Thrasher, J. T. Hartness, N. J. Johnston, R. M. Baucom, J. M. Marchello and M. K. Hugh, Proceedings of the 4th NASA Advanced Composites Technology Conference, (1993).

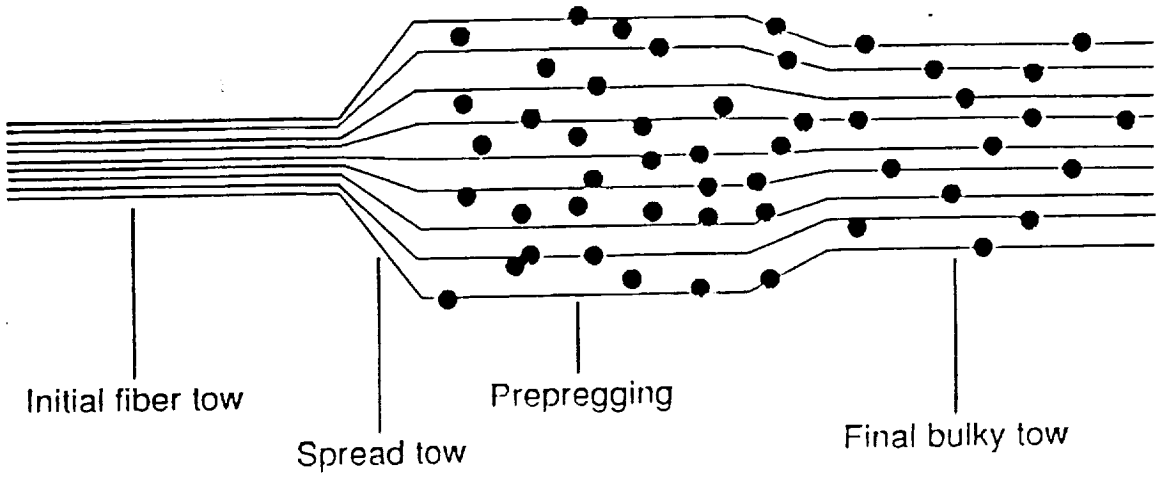

FIGURE 1. Schematic of the acquisition of bulk during the powder prepregging process.

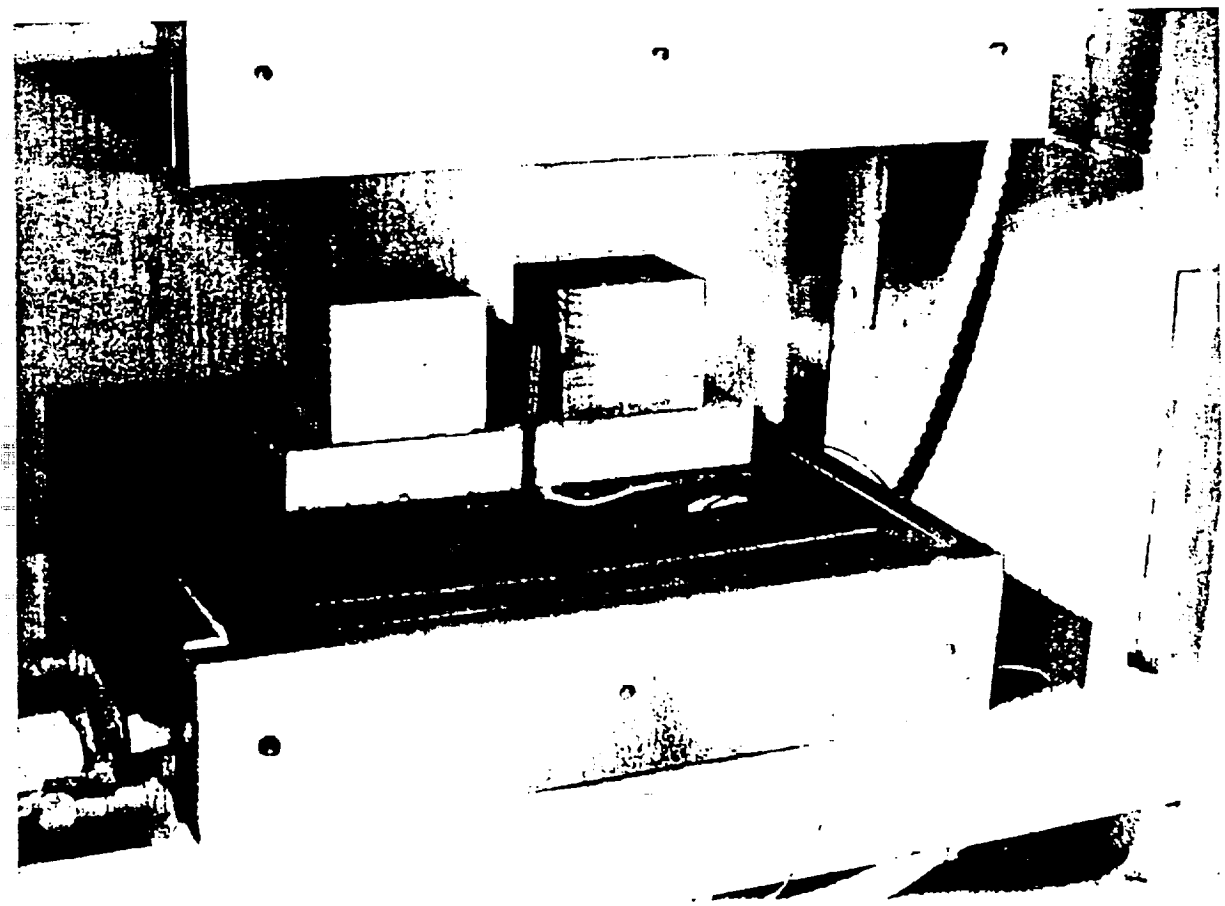

FIGURE 2. Experimental setup showing the skin of the T-stiffened panel being debulked using aluminium and wooden blocks and a heated press.

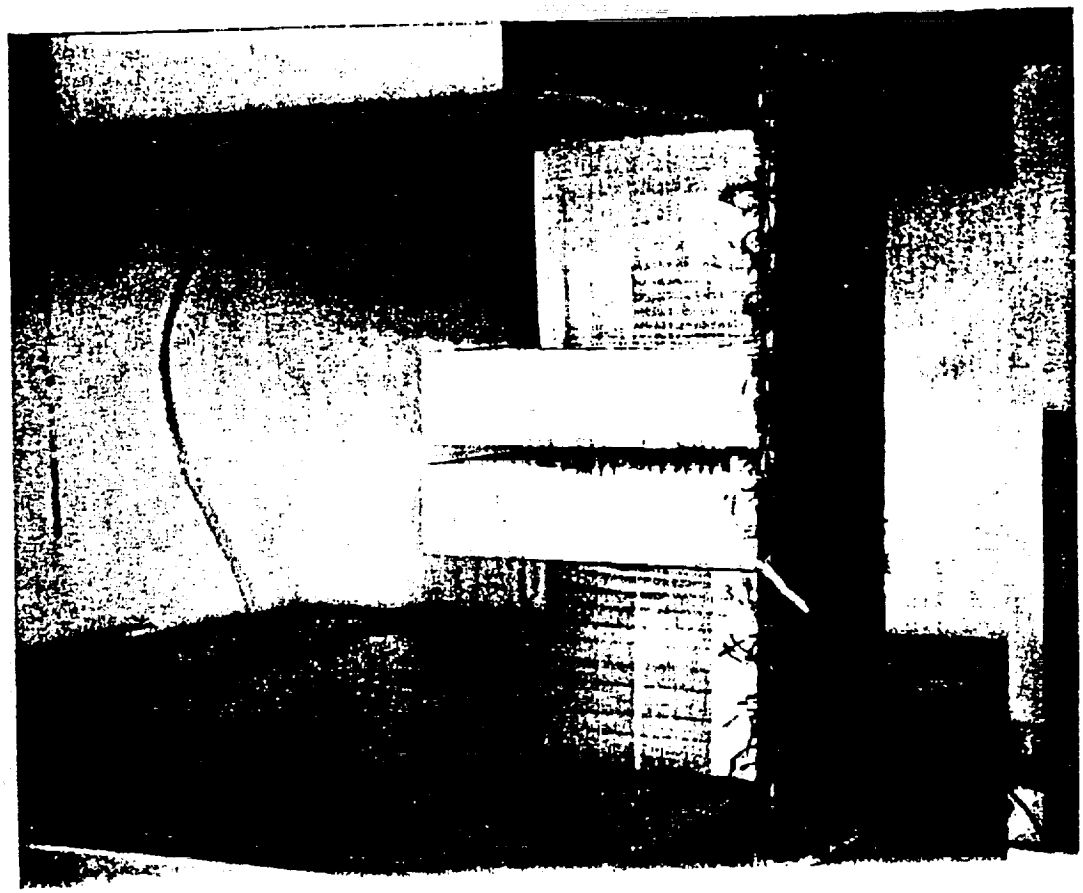

FIGURE 3. Experimental setup showing the stiffener being debulked using aluminium and wooden blocks and a heated press.

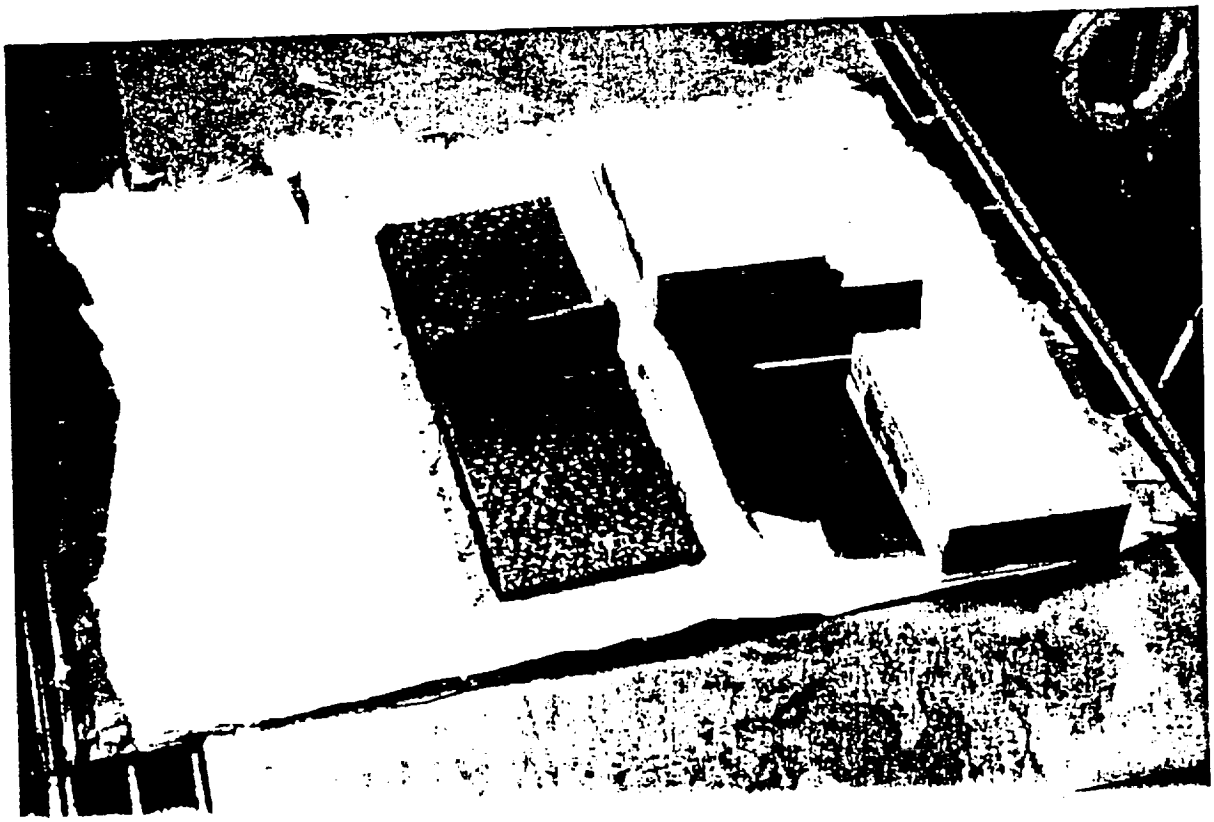

FIGURE 4. Photograph of the combination of hard and soft tooling used for final consolidation of the T-stiffened panels.

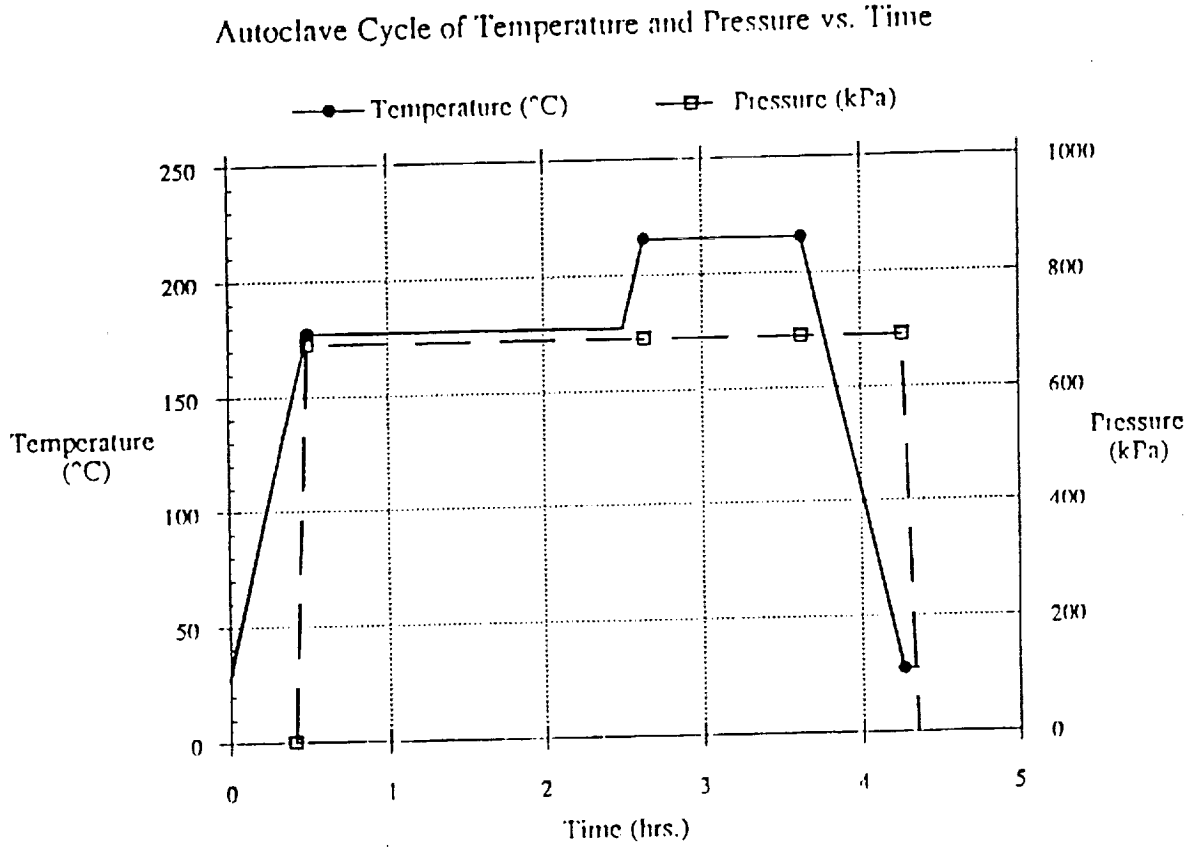

FIGURE 5. Final consolidation cure cycle for 3D woven T-stiffened panel made from epoxy powder-coated towpreg.

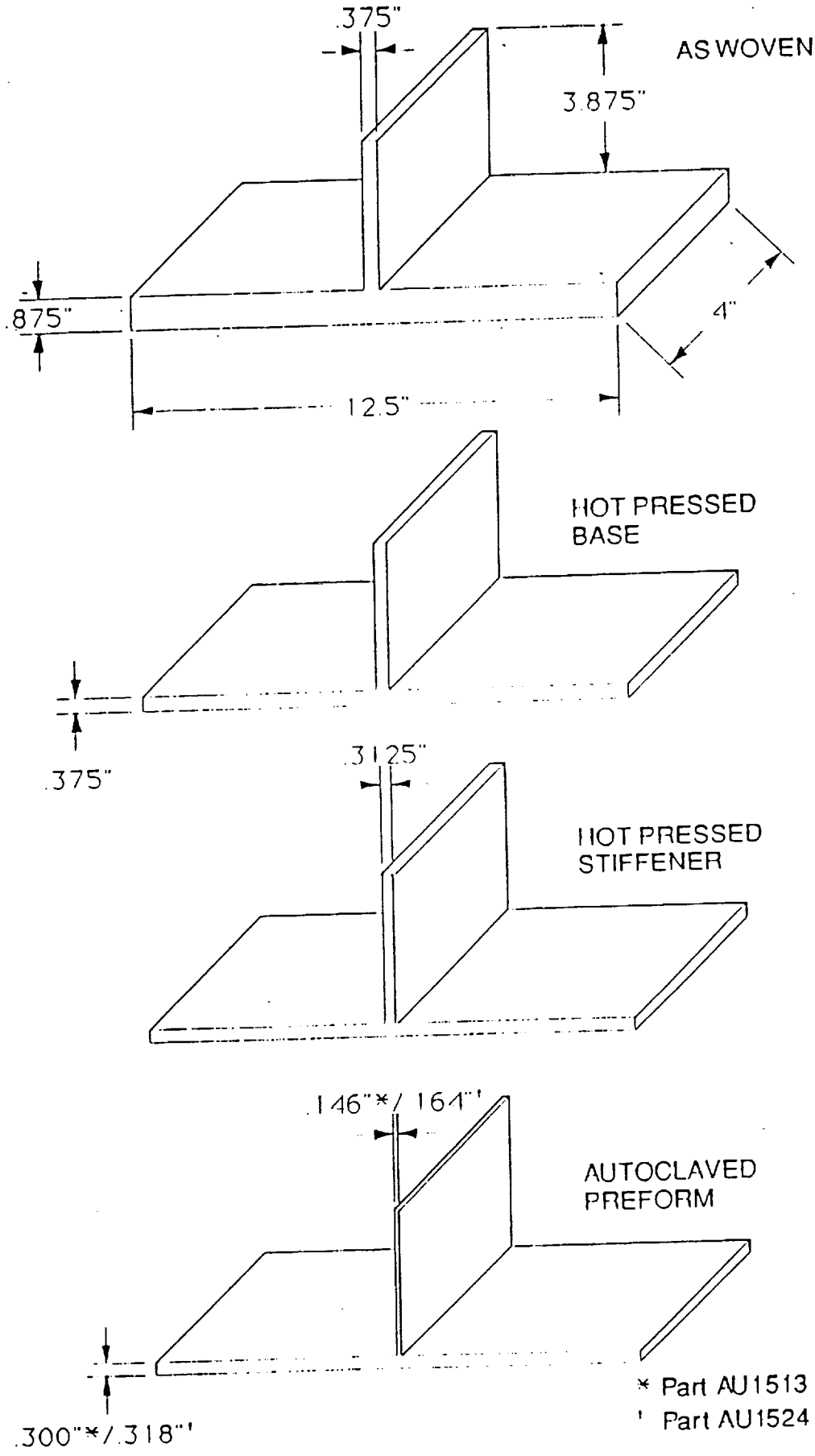

FIGURE 6. Dimensions for the T-stiffened panel taken during the debulking process.

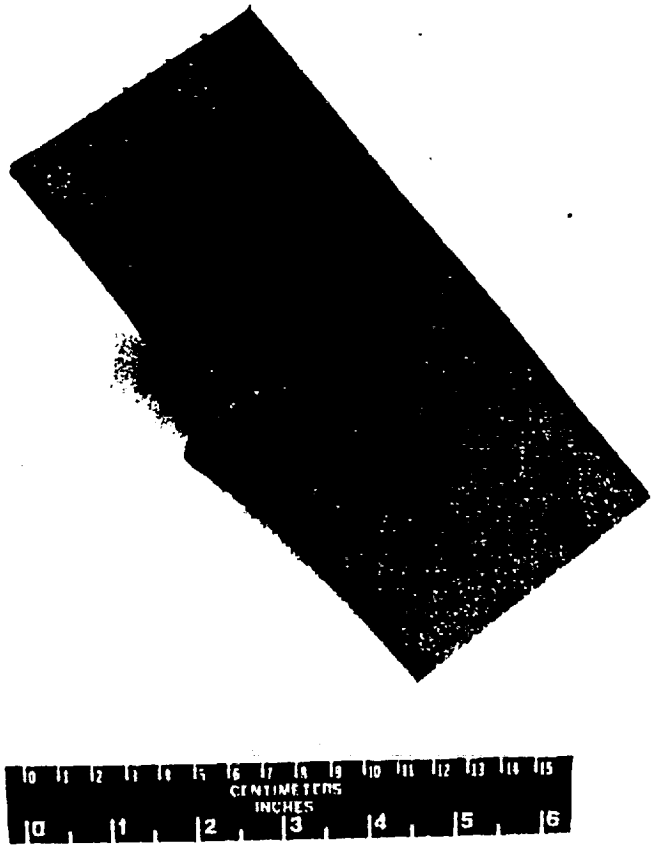

FIGURE 7. Bottom view of the first part (AU1513) exhibiting a dimple at the skin/stiffener intersection.

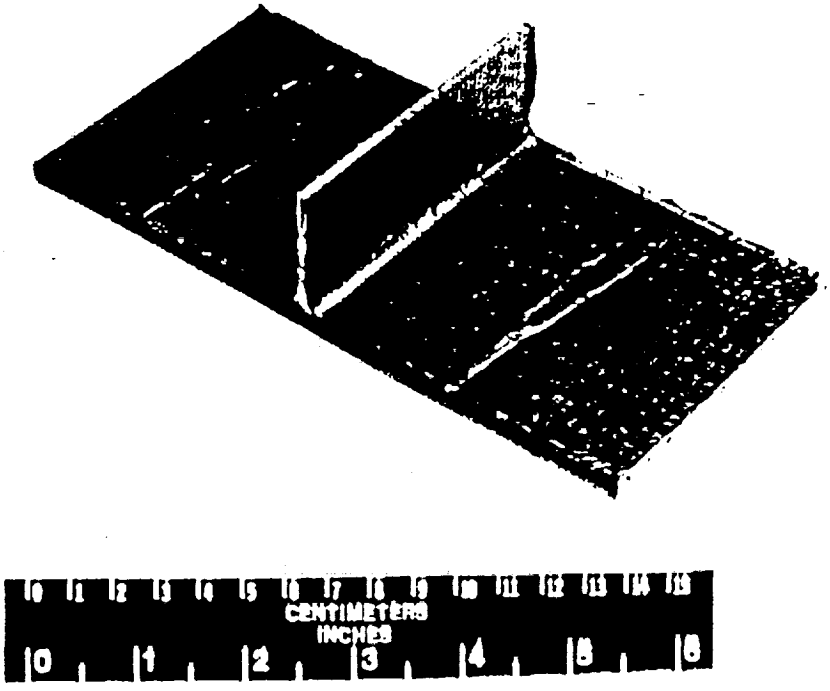

FIGURE 8. Top view of the first part (AU1513) exhibiting wrinkles on the skin surface.

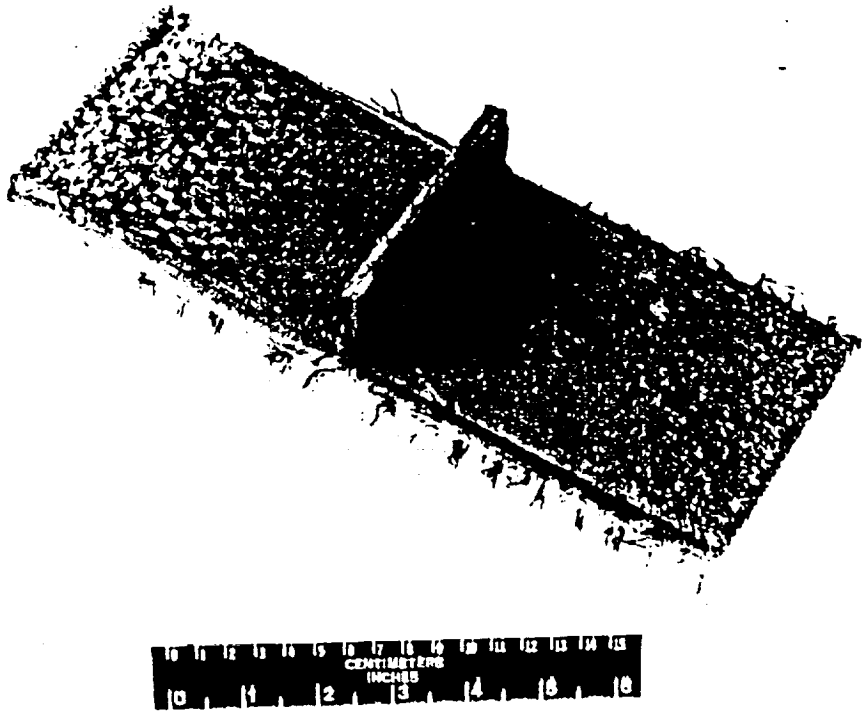

FIGURE 9. Photograph of the second part (AU1524).

July 14, 1993

Memorandum

To: D. Sandusky, J. Hinkley, R. Baucom and N. Johnston

From: J. Marchello

Subject: ATP Thermal Wave Bonding

For the past several months we have discussed ATP in-situ consolidation and the related thermal and diffusional processes. The purpose of this memorandum is to summarize our discussions as they relate to the autohesion kinetics studies we are undertaking.

ATP Thermal Wave Bonding Model

ATP Thermal Wave Bonding Model

1.0 Introduction

Ribbon-ribbon and ribbon-ply bonding during ATP occurs by the adhesion that takes place when the interfaces are above T_g. The array of ribbons being placed on the tool surface are heated as they leave the robot head and pass under the roller. During the time interval before the thermal wave decays below T_g, bonding occurs by polymer interfacial diffusion. The purpose of this report is to setforth equations which describe these processes.

The decaying temperature profile during ribbon placement is illustrated in the following figure that appeared in our October 1992 SAMPE paper. The bonding that occurs at a given interface is depicted in the second figure, which illustrates the increased bonding with subsequent passes over the point of interest. In this way, bond strength is expected to build up step-wise during the first and several subsequent passes.The goal of ATP in-situ consolidation is to achieve at least 80% of ultimate bond strength.

Analysis of the ATP thermal wave bonding process involves two steps: heating prior to gap closure; and, the heat conduction and autohesion kinetics that follows when the gap closes and the ribbon is in place. Thus, the model entails unsteady state heat transfer and diffusional adhesion of the polymer at the interface.

2.0 Pre-Gap Closure

As the ribbon passes from the robot head to the laydown surface, thermal energy is applied to the gap between the ribbons and the part/tool surface by hot gas and/or by radiation. The rate at which the surface and bulk of the material heats up is governed by Fourier's second law with appropriate boundary conditions for the convective and radiant surface heat fluxes.

The temperature profile of a ribbon heated by hot gas is described by solutions to Fourier's law of conduction:

$$\frac{\partial T}{\partial t} = \alpha \frac{\partial^2 T}{\partial y^2}$$

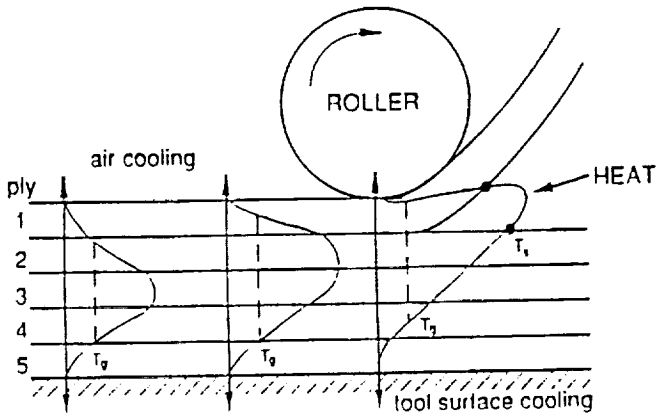

TEMPERATURE PROFILES DURING ATP

- Bonding at Ply 1 - Ply 2 interface is primarily by wetting
- Bonding at deeper ply interfaces is by diffusion when $T > T_g$

Figure 6. ATP Heat Wave Bonding Model.

Fig 2

THERMAL WAVE BONDING MODEL

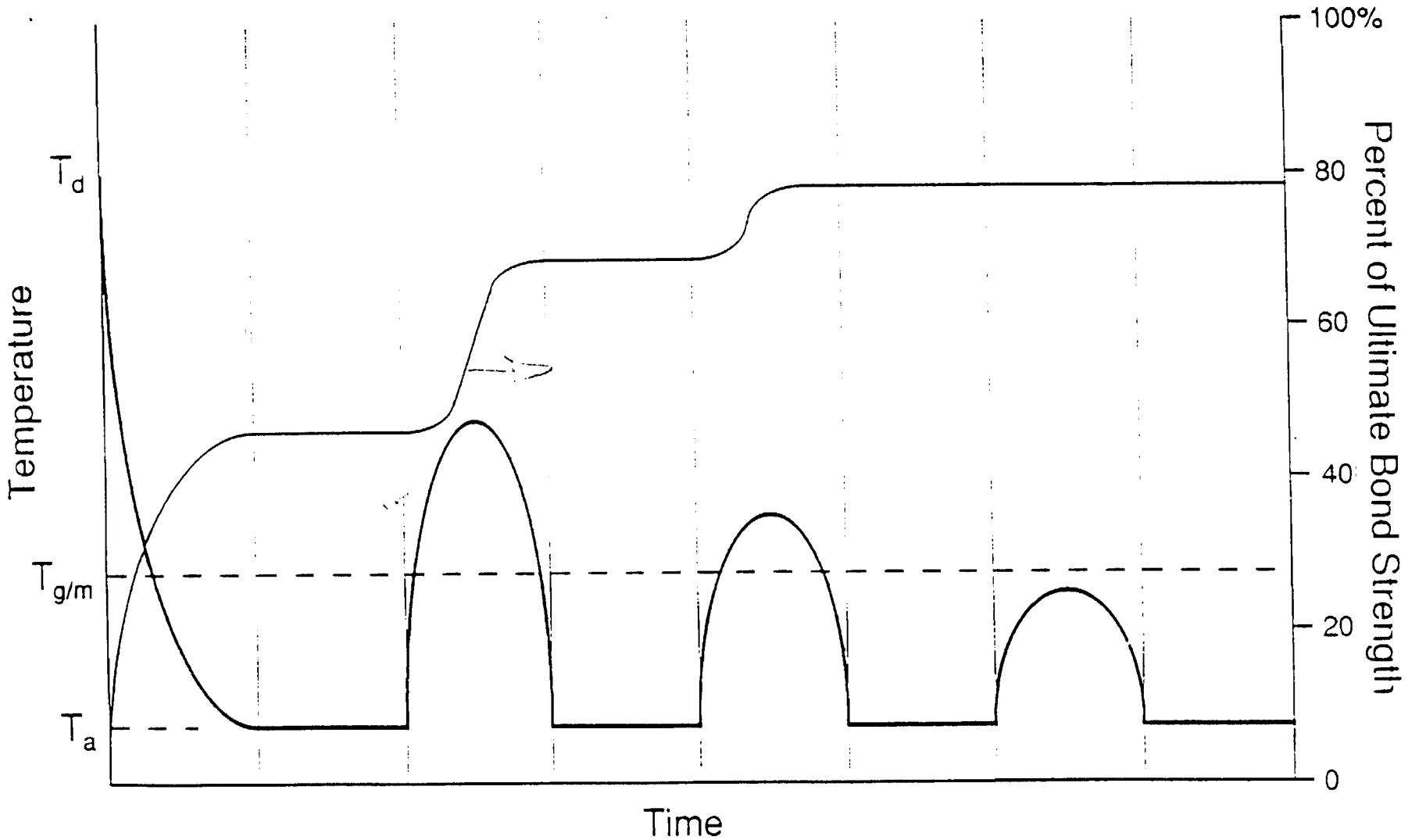

where T is the temperature, t is time, y is depth into the ribbon from the heated surface, and $\alpha = k/\rho C_p$ is the thermal diffusivity of the ribbon.

Three boundary conditions are needed for solution of this equation, one for time and two for position. For the time condition. assume that the ribbon is initially at the air temperature, $T(0,y) = T_a$. The two y boundry conditions describe the heat flux from the gas to the ribbon and the cooling on the back side of the ribbon. They are as follows.

2.1 Heat Transfer to the Ribbon

At the hot gas side of the ribbon in the gap

$$q_g = -k \frac{\partial T(t,0)}{\partial y} = h_g [T_g - T(t,0)]$$

where: q_g is the heating flux; k is the thermal conductivity of the ribbon; $\frac{\partial T(t,0)}{\partial y}$ is the temperature gradient at any time at the surface, $y = 0$; h_g is the convective heat transfer coefficient of the hot gas; T_g is the gas temperature; and, $T(t,0)$ is the ribbon surface temperature.

Note that the ribbon surface temperature should be maintained below the thermal decomposition temperature of the polymer in the ribbon, T_d. Operating with $T(t,0) = T_d$ represents the highest heating rate attainable without damaging the ribbon.

2.2 Heat Transfer from the Ribbon

At the air cooled backside of the ribbon

$$q_a = -k \frac{\partial T(t,\ell)}{\partial y} = h_a [T(t,\ell) - T_a]$$

where: q_a is the cooling flux; $\frac{\partial T(t,\ell)}{\partial y}$ is the temperature gradient at any time at the air side, $y = \ell$, of the ribbon; h_a is the convective heat tansfer coefficient of the air; $T(t,\ell)$ is the ribbon surface temperature on the air side; and, T_a is the air temperature.

2.3 Part heating

Heat enters the previously placed material, and/or part, according to the same conduction expression

$$\frac{\partial T}{\partial t} = \alpha \frac{\partial^2 T}{\partial y^2}$$

In this case, the boundary condition at the surface in contact with the hot gas is

$$q_g = k \frac{\partial T(t,0)}{\partial y} = h_g [T_g - T(t,0)]$$

which indicates that heat is transferred in the negative y direction into the part.

2.4 Tool Heating and cooling

At the backside of the part, $y = -L$, at the tool surface, the boundary conditions depend on whether the tool is cooled and how thick the previously placed material is. For example, once a number of plies have been laid down, the placed material may appear infinitely thick, in that the thermal wave does not extend to the part. Then, the boundary condition would be, $L \to -\infty$,

$$T(t, -\infty) = T(0, -y)$$

which says that during the brief placement interval there is no temperature rise deep down in the material, and so the temperature deep in the material is the initial part temperature, $T(0,-y)$.

On the other hand, for a metal tool, when only a few piles have been placed, the condition might be

$$T(t,-L) = T(0,-L) = T_{tool}$$

which says the tool is a highly conductive heat sink that stays at its intial temperature, $T(0,-L)$.

There are several other options for the tool surface boundary condition. In the general case of a tool of thickness L_T cooled by air on the back, non-placement, side the heat flux from the placed material to the tool would be

$$q_T = k \frac{\partial T(t,-L)}{\partial y} = k_T \frac{\partial (t,-L)}{\partial y}$$

which says the conduction rate across the part-tool interface, $y = -L$, are equal. Then, at the air side of the tool, of thickness L_T,

$$q_{aT} = k_T \frac{\partial}{\partial y} T(t, -L-L_T) = h_{aT} [T(t, -L-L_T) - Ta]$$

where $T(t,-L-L_T)$ is the temperature of the tool at its air surface.

2.5 Temperature Profiles

Solutions to the above sets of differential equations and boundary conditions form a family of equations for the temperature as a function on time and position. The shape of these curves depends upon the properties of the materials and the convective heat transfer rates. The pre-gap closure temperature profile in figure one illustrate the general form of these equations.

As shown in the first attachment, a number of applicable solutions to the above problems have been worked out using operational and series techniques. To pursue the theoretical analysis further, it will be necessary to put physical property data into these solutions and calculate the appropriate temperature profiles in the ribbon and part.

An alternative approach, and perhaps easier to do, would be use the above relationships to set up finite element numerical methods to calculate the profile. This would involve obtaining computer programs for making the calculations that enable the plotting of the profiles. Again, physical property data would be required.

3.0 Post-Gap Closure

Once the ribbon-part gap closes, the temperature profile decay as heat is transfered into the part and to the air and tool. This is illustrated in figure 1 by the temperature profiles after the roller passes. During this time period, diffusion bonding occurs at the interface as illustrated on figure 2.

3.1 Thermal Wave Decay

From the time of gap closure the temperature profile, $T(t_c, y)$, changes according to the following set of relationships

$$\frac{\partial T}{\partial t} = \alpha \frac{\partial^2 T}{\partial y^2}$$

Initially the temperature profile is the solution to the pre-gap case, when $t = t_c$, the time at which closure occurs.AS shown in the first attachment, this is a series function of y.

Decay of this initial profile is governed by conduction with the following boundary conditions for cooling.

At the cool air surface

$$q_a = -\frac{k\,\partial T(t,\ell)}{\partial y} = h_a\left[T(t,\ell) - T_a\right]$$

and at the part surface, section 2.3,

$$q_T = k\frac{\partial T(t,-L)}{\partial y} = k_T\frac{\partial T}{\partial y}(t,-L)$$

and

$$q_{aT} = k_T\frac{\partial T(t,-L-L_T)}{\partial y} = h_{a_T}\left[T(t,-L-L_T) - T_a\right]$$

Note, that as originally set up, y is negative into the laid down material and into the part. The direction of y probably should be changed for convenience when numerical calculations are made with these equations.

During the post-gap closure thermal decay, time starts at $t = t_c$ and all solutions involve $t \geq t_c$. This, of course, can be handled algebraically by introducing a new time variable $\Theta = t - t_c$. Then the temperature profiles would be found among those presented in the first attachment. Again, it may be easier to work out finite element computer solutions rather than deal with these complex series expressions.

3.2 Autohesion Bonding

As illustrated in the second figure, interfacial bonding occurs by diffusion when the temperature is above T_g. The increase in bond strength depends on the diffusion kinetics of the polymer and follows an Arrhenius temperature relationship.

Thus, to calculate the increase in bond strength requires a knowledge of the time-temperature relationship of the interface during placement and subsequent passes over the surface. It also requires a knowledge of the diffusion rate as a function of time and temperature.

In the above sections the procedures for determining the time-temperature relationship were described, For autohesion bonding, these equations with $y = 0, -\ell, -2\ell$, etc. would be needed. Once these interface time-temperature expressions have ben obtained, they would be used with the autohesion diffusion relationship to predict bonmd strength as a function of time.

4.0 Autohesion kinetics

Diffusional bonding (crack healing) at the ply-ply interface has been studied by a number of investigators. As shown in the other attachments, the current theory predicts a one-fourth power dependence on time for isothermal bonding. The limited amount of data available, generally support the reptation theory, and deal with time periods much greater those of interest in ATP in-situ consolidation.

In the case of ATP in-situ consolidation, the time intervals are less than one second. Thus, neither the theory nor available data may be applicable. For this reason we have initated an experimental study of short-time autohesion kinetics.

4.1 Rate Equation

Autohesion theory predicts that, at a constant temperature above T_g, ply-ply interfacial bonding increases as the one-fourth power of the time of contact. That is

$$B(t) = B(\infty)\left(\frac{t}{t_0}\right)^{1/4}$$

where $B(t)$ is the strength of the interlaminar bond after a time t of contact, $B(\infty)$ is the ultimate bond strength, and t_0 is an autohesion or reptation time constant related to the polymer properties, such as diffusivity and molecular weight.

The bonding time constant, t_0, would be expected to have an Arrhenius type dependence on temperature. That is

$$t_0 = A\, e^{-E/RT}$$

or

$$\log(t_0) = \log(A) - E/RT$$

An interlaminar bonding strength-time expression should show no bonding initally and should level off at $B(\infty)$ after a long time, $t \to \infty$. The above reptation model does not fit the long time condition. It fits the initial condition, but may not accurately describe the short-time situation.

The rate of bonding for this model is

$$\frac{\partial B(t)}{\partial t} = \left[\frac{1}{4} B(\infty)\, t_0^{-1/4}\right] t^{-3/4}$$

This equation indicates the rate is infinite at $t = 0$ and decreases to zero for long times. This seems reasonable. A key point in achieving ATP in-situ consolidation is whether this rapid initial bonding occurs each time the interface rises above T_g. If so, as shown in the second figure, the bond strength goal of 80 % could be reached in a few passes.

4.2 ATP Bonding Integrals

During ATP the interlaminar interface is not isothermal. Thus, it is necessary to combine the expressions discussed earlier for the time-temperature equations of the interfaces with the bonding rate equation and integrate over the time interval above T_g. This would need to be done for each heating sequence.

As pointed out in section 3.1, and illustrated in the second figure, upon gap closure, temperature decays in accordance with the thermal conductivity of the composite and the rates of cooling provided at the air and tool surfaces. Thus, the heat transfer analysis provides a functional expression for the interlaminar temperature as a function of time, $T(t, y)$. This equation is only needed at $y = 0$, ℓ, 2ℓ, etc. In general it would be $T(t, n\ell)$ (assuming the y coordinate is now positive into the part). Here n is the ply-ply number, $0, 1, 2,$ etc.

The growth in bond strength, at ply interface n, during ATP heating time interval Δt_i is given by the integral

$$B_n(\Delta t_{n,i}) = \int_{\Delta t_{n,i}} \frac{\partial B_n(t)}{\partial t} dt$$

where Δt_{ni} is the time the interface spends above T_g during the pass over the point of interest.

As shown in the second figure, for the placement interval $i = 0$, at $n = 0$, and $y = 0$, the interface begins, $t = 0$, above T_g. After a time τ_g the temperature would have decayed to T_g. THis time would need to be calculated from the general equation $T(t, 0)$ and would be $\Delta t_{0,0}$.

For the interface at $n = 1$, $y = \ell$, as shown in the second figure, the temperature rises above T_g at some time t_{g10} and then decays back to T_g at some time later t_{g11}. Then $\Delta t_{10} = t_{g11} - t_{g10}$. Both t_{g11} and t_{g10} would be determined from the general equation $T(t, \ell)$. Similar calculations would apply for the

deeper plies. In this way, the time intervals, $\Delta t_{m,i}$, for the above integration could be established.

Using the equations in section 4.1 for the bonding rate as a function of time and temperature gives

$$\frac{\partial B_n(t)}{\partial t} = \frac{1}{4} B(\infty) A^{1/4} \left[e^{-E/4RT(m,i)} \right] t^{-3/4}$$

Substituting into the integral

$$B_n(\Delta t_{m,i}) = \frac{1}{4} B(\infty) A^{1/4} \int_{\delta t_{m,i}} e^{-E/4RT(t,m,i)} t^{-3/4} dt$$

This is the general expression for the step increases in bonding strength for the thermal bonding wave model. It uses the time-temperature expression, $T(t,ml)$, from section 3.1 and the rate equation from section 4.1 and would predict the stepwise increase in interlaminar strength illustrated in the second figure.

4.3 Observations

In conculsion, we have a theoretical model for the ATP thermal wave increase in ply-ply, or ribbon-ribbon, bonding. While it is complete in nearly every sense of physical description, it is exceedingly complex. One could obtain polymer properties, air and tool cooling information, and with the air of a computer calculate theoretical predictions for the curves shown in the two figures.

One matter not dealt with in this analysis is the possible effect of initial unevenness of the surfaces. An important consideration during initial gap closure is the polymer flow that may be required to obtain complete interlaminar contact. The model will need to have this aspect built into it, should we decide to properly model the short time mechanisms of interlaminar bonding.

From a practical point of view, it does not seem necessary to work out these involved solutions. It appears sufficient to acknowledge that we understand the theoretical background for ATP in-situ consolidation. It seems apropriate to conduct small scale experiments on short-time ribbon bonding kinetics and to apply this experimental information in the design of robot head equipment for ATP in-situ consolidation. This is the rationale for the autohesion kinetics studies we are undertaking.